Joint Experiments on the Tokamaks CASTOR and T-10

G Van Oost[a], M Gryaznevich[b], E Del Bosco[d], A Malaquias[f], G Mank[f], M Berta[e, m], J Brotankova[c], R Dejarnac[c], E Dufkova[c], I Duran[c], M Hron[c], P Peleman[a], J Sentkerestiova[c], J Stöckel[c], B Tál[e], V Weinzettl[c], J Zajac[c], S Zoletnik[e], V Budaev[k], N Kirneva[k], G Kirnev[k], B Kuteev[k], A Melnikov[k], M Sokolov[k], V Vershkov[k], I El Chama Neto[o], J Ferreira[d], R Gonzales[n], C R Gutierrez Tapia[r], H Hegazy[h], P Khorshid[l], A W Kraemer-Flecken[p], L I Krupnik[s], Y Kuznetsov[g], A M Marques Fonseca[q], A Ovsyannikov[i], L Ruchko[g], E Sukhov[i], A Singh[j], V Soldatov[p], A Talebitaher[l], , G M Vorobjev[i]

Dep. of Applied Physics, Ghent Univ., Belgium; bEURATOM/UKAEA Fusion Association, Culham SC, Abingdon, UK; cInstitute of Plasma Physics, Association EURATOM/IPP, Czech Rep.; dINPE, São José dos Campos, Brazil; eKFKI-RMKI, Association EURATOM, Budapest, Hungary; fIAEA, NAPC Physics Section, Vienna, Austria; gInstitute of Physics, Univ. of São Paulo, Brazil; hEAEA, Cairo, Egypt; iSaint Petersburg State Univ., Russia; jPlasma Physics Lab., Univ. of Saskatchewan, Canada; kRRC "Kurchatov Institute", Moscow, Russia; lPlasma Physics Research Center, Teheran, Iran; mSzéchenyi István Univ., Association EURATOM, Győr, Hungary; nCICATA-IPN, Mexico; oUniv. Tuiuti Paraná, Brazil; pForschungszentrum, Julich, Germany; qIST, Lisbon, Portugal; rININ, Mexico; sPhys-Tech Inst., Kharkov, Ukraine

Abstract. Small tokamaks may significantly contribute to the better understanding of phenomena in a wide range of fields such as plasma confinement and energy transport; plasma stability in different magnetic configurations; plasma turbulence and its impact on local and global plasma parameters; processes at the plasma edge and plasma-wall interaction; scenarios of additional heating and non-inductive current drive; new methods of plasma profile and parameter control; development of novel plasma diagnostics; benchmarking of new numerical codes and so on. Furthermore, due to the compactness, flexibility, low operation costs and high skill of their personnel small tokamaks are very convenient to develop and test new materials and technologies. Small tokamaks are suitable and important for broad international cooperation, providing the necessary environment and manpower to conduct dedicated joint research programmes. In addition, the experimental work on small tokamaks is very appropriate for the education of students, scientific activities of post-graduate students and for the training of personnel for large tokamaks. The first Joint (Host Laboratory) Experiment (JE1) has been carried out in 2005 on the CASTOR tokamak at the IPP Prague, Czech Republic. It was jointly organized by the IPP-ASCR and KFKI HAC, Budapest, involved 20 scientists from 7 countries and was supported through the IAEA and the ICTP, Trieste. The objective of JE1 was to perform studies of plasma edge turbulence and plasma confinement. Following the success of JE1, JE2 has been performed on T-10 at RRC "Kurchatov Institute" in Moscow; 30 scientists from 13 countries participated in this experiment. This experiment aimed to continue JE1 turbulence studies, now extending them to the plasma core. Results of JE1 and JE2 will be overviewed and compared.

Keywords: Tokamaks, Diagnostics, Edge physics, Plasma turbulence.
PACS: 52.35.Ra; 52.55.Fa; 52.70.DS; 52.70.KZ

CP996, *Plasma and Fusion Science*, edited by C. Varandas and C. Silva

INTRODUCTION

In the framework of the IAEA Coordinated Research Project (CRP) on "Joint Research Using Small Tokamaks" [1], Joint Experiments (JEs) have been carried out on the CASTOR tokamak at IPP Prague, Czech Republic in 2005 and on T-10 tokamak at RRC "Kurchatov Institute", Moscow, Russia in 2006. These JEs involved more than 40 scientists from 14 countries, coordinated and co-supported by IPP Prague, KFKI-RMKI Budapest, RRC "Kurchatov Institute" Moscow, IAEA and ICTP, Trieste. The experimental programme was aimed to diagnose and characterize the core and the edge plasma turbulence in a tokamak in order to investigate correlations between the occurrence of transport barriers, improved confinement, electric fields and electrostatic turbulence using advanced diagnostics with high spatial and temporal resolution. The edge plasma in a small and a large scale experiments has many similar features, and the results obtained through detailed measurements in the small CASTOR device are in many aspects still relevant to those in larger tokamaks. This has been demonstrated at the 2nd JE on T-10. During experiments on CASTOR, electric fields were generated by biasing an electrode inserted into the edge plasma to modify the turbulence and transport in this region. During experiment on T-10, clear correlation between fluctuations in the core plasma potential and density has been observed. Main results of these two experiments will be overviewed and compared.

The understanding and reduction of turbulent transport in magnetic confinement devices is not only an academic task, but also a matter of practical interest, since high confinement is chosen as the regime for ITER and possible future reactors because it reduces size and cost. Generally speaking, turbulence comes in two classes: electrostatic and magnetic turbulence. Over the last decade, step by step new regimes of plasma operation have been identified, whereby turbulence can be externally controlled, which led to better and better confinement. About a decade ago local zones (called internal transport barriers, ITBs) with reduced transport were discovered in tokamaks. These ITBs can act on the electron and/or ion fluid.

The physical picture that is generally given is that by spinning up the plasma, it is possible to create flow velocity shear large enough to tear turbulent eddies apart before they can grow, thus reducing electrostatic turbulence. This turbulence stabilization concept has the universality, needed to explain ion transport barriers at different radii seen in limiter-and divertor tokamaks, stellarators, reversed field pinches, mirror machines and linear devices with a variety of discharge- and heating conditions and edge biasing schemes. The electron heat conduction, however, which normally is one to two orders above the collisional lower limit, remained strongly anomalous also in the regime with suppressed electrostatic turbulence. In that case it became the dominant heat loss channel. From this, it is conjectured that magnetic turbulence drives the anomalous electron heat conduction. Experiments at the T-10 tokamak which specifically addressed the electron thermal transport properties of the plasma have strongly corroborated this conjecture and demonstrated that flow velocity shear is not the reason of confinement increase in the electron ITB region , but most likely a consequence of ITB formation. It was shown that e-ITBs form when contact between turbulent cells located at rational surfaces is broken. This may be seen at low number rational surfaces (m/n= 1/1, 2/1, 3/2 and so on).

Although turbulence measurements have been performed on many magnetic confinement devices during the last decades, the additional insight gained from these experiments is relatively limited. This can be attributed to a number of reasons:

- Firstly, only a very coarse spatial resolution was achieved in many measurements of electric fields and turbulence.
- Secondly, simultaneous measurements of different fluctuating quantities (temperature, density, electric potential and magnetic field) at the same location, needed for a quantitative estimation of the energy and particle transport due to turbulence were only performed in a very limited number of cases.
- Thirdly, theoretical models were often only predicting the global level of turbulence as well as the scaling of this level with varying plasma parameters.

Improvement and development of some diagnostics (such as heavy ion beam probe, correlation reflectometry, Mach probes and fast bolometers) were necessary for the successful execution of the project The most important results obtained in the investigations of the physical mechanisms underlying different types of transport barriers and of turbulence during JE1 on CASTOR and JE2 on T-10 are presented.

EDGE PLASMA STUDIES ON CASTOR

The particular feature of this experiment is the exploitation of unique diagnostics to study the physics of the edge plasma in detail [2]. During the experiments, electric fields were generated by biasing an electrode inserted into the edge plasma to modify the turbulence and transport behaviour in this region. The CASTOR tokamak (R= 0.4 m, a= 0.085 m, Bt < 1.5 T, Ip < 25 kA, ΔT < 50 ms, 0.5< $n_e(10^{19}$ $m^{-3})$ <3.0, $T_e(0)$ < 200 eV) is equipped with a circular cross section poloidal limiter, and with a standard set of diagnostic tools. During these joint experiments the available diagnostic systems were two bolometric arrays for the fast measurement of radiation losses, Langmuir probe arrays for edge plasma monitoring in radial and poloidal directions, directional probes (Gundestrup) for parallel and perpendicular plasma flow determination, and a full poloidal array of magnetic pick-up coils and Hall sensors for plasma position monitoring. The H_α diagnostic was located at the top of the vessel at the same toroidal location of the rake probes to monitor the radiation due to recycling.

The edge plasma and the electrostatic turbulence were characterized using a radial array consisting of a double rake probe with 16 Langmuir tips each (the radial separation between two adjacent pins is 2.5 mm). The time evolution of the radial profiles of electron temperature and density was measured during a single shot. Furthermore, from the time shift between the signals of two poloidally separated tips it was possible to measure the poloidal velocity of fluctuating density and plasma floating potential structures. Since these time shifts were typically lower than the sampling rate (1μs), two statistical techniques were developed allowing the determination of the correlation length and phase velocity of potential fluctuations during a single shot: (i) polynomial curve fitting (fitting the cross-correlation by some polynomial function), and (ii) linear fitting of the phase function of the cross-power

spectral density. Both techniques provided similar results, as illustrated in Fig.1. Both methods diverge in the proximity of the Last Closed Flux Surface (LCFS), which is associated with the maximum of the floating potential seen in the left graph of Fig.1.

However, the position of the velocity shear layer (VSL) can be identified with a precision of ~1 mm. From the gradient of floating potential (dashed line in the left graph of Fig. 1.), the phase velocities were roughly estimated as $v_{ph} = E_r/B$, where E_r is estimated as grad Φ_f, neglecting the gradient of the electron temperature. In the right graph, the velocities are depicted as three horizontal lines (in the region 50<r<60mm v_{ph}=-1.4km/s, for 60<r<70 mm v_{ph}=-3.3 km/s, and for 70<r<90 mm v_{ph}=1.3 km/s). It is evident that experimental points are above these lines, which implies that the electron temperature gradient cannot be fully neglected, if a precise comparison of the phase and ExB velocity is required. Finally, it is interesting to note that the phase velocity of density fluctuations is systematically lower than that of potential fluctuations. The explanation of this observation requires more analysis. Furthermore, from the spatio-temporal behaviour of cross-correlation functions of radially separated tips, a radial size of the fluctuating structures of about 1 cm was determined during this experimental campaign.

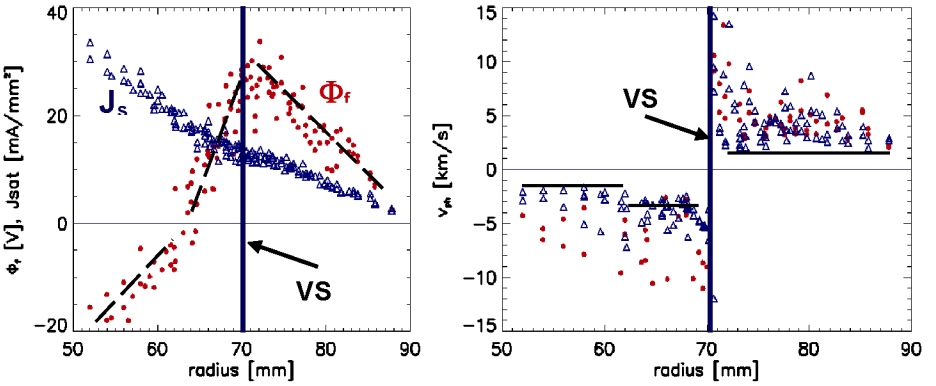

FIGURE 1. Left graph: Radial profiles of floating potential Φ_f (red circles), and density of ion saturation current J_{sat} ($J_{sat}=I_{sat}/A$, A is 2π x radius x length of the probe). Right graph: Phase velocities of fluctuations obtained from Φ_f (red circles), and J_{sat} (blue triangles). Horizontal lines in the right panel show velocities calculated from the gradient of Φ_{fl}.

Figure 2 further illustrates the influence of the positive biasing on the radial profile of edge plasma parameters. The radial profiles of the floating potential ϕ_f, radial electric field E_r and its shear dE_r/dr, and ion saturation current I_s are obtained by averaging over a time window of 4 ms before (open symbols) and during (filled symbols) the biasing phase. Here, E_r is calculated directly from the radial derivative of ϕ_f measured at r=60mm on two adjacent pins neglecting the contribution from the T_e gradient, and therefore underestimating E_r slightly. The radial position of the LCFS is around r_{LCFS} = 66 mm (indicated by the dashed-dotted line in the figures). During the biasing phase, the radial dependence of ϕ_f is strongly modified as shown in Fig. 2(a),

leading to a narrow positive and single-peaked E_r structure with a maximum of 11 kV/m at $r \approx 61$ mm, just inside the LCFS ; see Fig. 2(b). As a consequence, a strong positive (~1.3MV/m^2) and negative (~ -1MV/m^2) E_r shear are generated inside and across the LCFS, respectively, as shown in Fig. 2(c). The maximum shear rate of the $E_r \times B$ flow, $\tau_s^{-1} \propto dv_{\vec{E}\times\vec{B}}/dr$, is thus about 1-1.3$\times 10^6$ s^{-1}. On the other hand, the decorrelation rate of local turbulence scattering, τ_{c0}^{-1}, calculated from the e-folding time of the autocorrelation function of I_s fluctuation data detected before biasing, gives $\tau_{c0}^{-1} = 1.6\times 10^5$ s^{-1}. Hence, the flow shear rate exceeds significantly the turbulence scattering rate and thus suppresses turbulence and turbulent transport. The reduction in I_s and ϕ_f fluctuations during biasing has been observed in the experiments. The reduced turbulent transport leads to the formation of an edge pedestal and thus to a steepening of the edge density profile during biasing, as shown in Fig. 2(d). It can be concluded that a clear and reproducible transition to improved confinement is induced by the edge electrode biasing along with the creation of a particle edge transport barrier just inside the LCFS. This barrier is characterised by (i) a substantial increase of the edge density gradient; (ii) a reduction in recycling indicated by a drop in H_α signal; (iii) a substantial increase of the global particle confinement time; (iv) suppression of the density and potential fluctuation level.

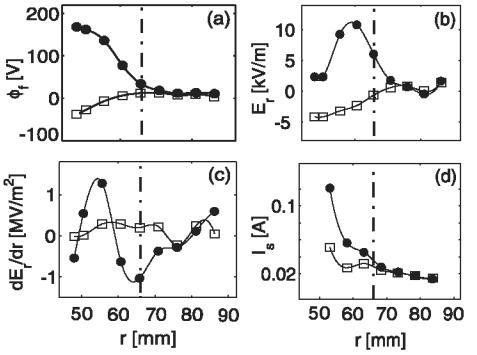

FIGURE 2. Radial profiles of (a) the floating potential ϕ_f, (b) the radial electric field E_r, (c) the E_r shear, and (d) the ion saturation current I_s averaged over 4 ms before (open symbols) and during (filled symbols) biasing. The vertical dashed-dotted line marks the position of the LCFS.

Flow measurements were performed using a Gundestrup probe with 8 collectors [3]: the time evolution of the radial profiles of floating potential, radial electric field, parallel and perpendicular Mach numbers was obtained in the biased and ohmic phases of a single discharge. It is found that not only the perpendicular, but also the parallel flow increases during biasing. The radial flow profiles were measured by a shot-to-shot scan in reproducible discharges, see Fig.3.

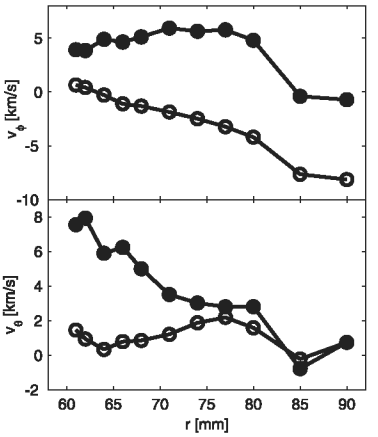

FIGURE 3. Radial profiles of the toroidal velocity v_ϕ and poloidal velocity v_θ averaged over 4 ms before (open circles) and during (filled circles) biasing..

Two arrays of fast AXUV-based bolometers (A=advanced) with 16 and 19 channels were installed in the same poloidal cross-section of CASTOR in mutually perpendicular directions (from the LFS and bottom side) to monitor the radiated power profile. This arrangement with unique temporal resolution of 1 μs and spatial resolution of about 1 cm and a very high signal to noise ratio allowed a visualization of fine structures on the radiated power profile. First, the measured AXUV data are typically used to find the evolution of the total radiation, radiation peak position (shift), radiation FWHM and the brightness profile [4]. Afterwards, the data are separated into spatio-temporal components by the Singular Value Decomposition method (SVD). The analysis of the fluctuating part of raw fast bolometric data were processed by subtracting the mean value. The data are chord integrated, thus the result does not correspond to the evolution of single local turbulent events but with their sum along the whole chord. By the autocorrelation analysis, the event frequency can be obtained from the periodicity of the auto-correlation function. The cross-correlation of one channel with neighbouring ones in principle gives the velocity and the direction of the movement, while the cross-correlation with a perpendicular bolometric chord gives the localization of the event. As an illustration, the cross-correlation analysis (horizontal chord at 40 mm against bottom chords) of shot #26991 with a biasing period at 10-15 ms is shown in Fig.4. Prior to biasing, clear structures with repetition frequency about 30 kHz are present. During biasing, the periodicity is destroyed, but the surface near radius 50 mm shows a high level of correlation indicating the presence of a well-localized structure. A few milliseconds after the end of biasing, the periodicity is still not restored, however, a well-correlated, radially moving event is registered.

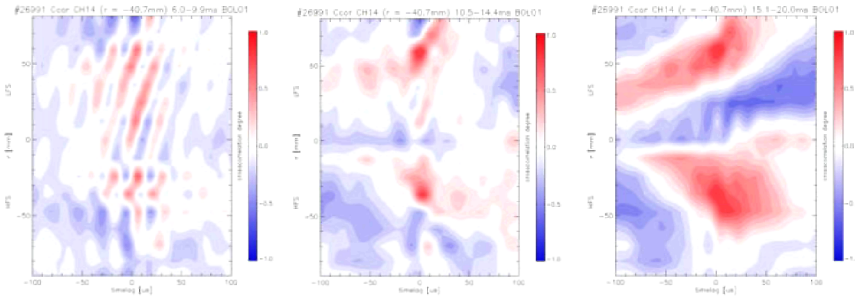

FIGURE 4. Cross-correlation between one horizontal chord at 40 mm against all bottom chords show moving structures in the shot #26991. Prior to biasing (left figure),the presence of the periodic events with frequency 30kHz and velocity 2.3 km/s are demonstrated. During biasing with biasing voltage +150V(middle figure), the surface near radius 50 mm shows a high level of correlation indicating the presence of well-localized structure . After biasing (right figure), a well-correlated, radially moving event is registered.

PLASMA POTENTIAL, RADIAL ELECTRIC FIELD AND TURBULENCE ROTATION IN T-10

The Heavy Ion Beam Probe (HIBP) is the only diagnostic, which is able to provide the plasma electric potential measurements and its fluctuations in the bulk plasma. The spontaneous changes of the edge plasma potential during L-H transition have been measured by HIBP in tokamaks, but the steady state edge profiles have not been reported so frequently. To probe the plasma core in the T-10 tokamak (R_0 =1.50 m, a = 0.30 m), Tl^+ ions were accelerated up to 260 kV. The recent modification of the beam lines and the entrance ports expands the HIBP observation area in the upper outer quadrant of the plasma cross-section. The plasma was limited by the movable rail limiter at alim = 0.27-0.3 m, and the circular limiter at ac lim = 0.33 m. HIBP was able to operate in the range of normalized radial $0.57< \rho<1.0$ (depending on B_t), providing the plasma potential profile along with the probing beam current Itot which represents the density profile [5]. The observed radial interval moves towards the plasma centre with decreasing Bt. The sample volume position in the plasma in a single discharge can be either fixed or scanned radially with a period of 10 ms, producing a series of profiles during a single shot. Sample volumes look like elliptical disks, approximately 1cm × 1.5 cm (radial) × 0.5 cm (thickness). The uncertainty in the sample volume position was up to 2 cm.

Core plasma turbulence was investigated using correlation reflectometer (CR) [6].The CR reflectometer system on T-10 had two antenna arrays, probing the plasma from the Low Field Side (LFS) and the High Field Side (HFS).As shown in Fig. 1 both arrays were located at the top of the plasma column shifted at ≈30° to both sides with respect to the vertical central line. All antennas were mounted at radius 41 cm and aligned to the centre of the vacuum vessel. The LFS array had 6 pyramidal horns with width 2.5 cm, height 4 cm and length 12 cm. The reflection of the O-mode with electric field vector of the launched wave parallel to the magnetic field was used. The

frequency range varied from 22 to 78 GHz corresponding to the densities in the reflection point ranging from 0.6×10^{19} m^{-3} to 7.5×10^{19} m^{-3}, enabling measurements over the whole plasma radius.

In the ohmically heated phase of the regime with on-axis ECR heating of low density plasma (B_0 = 2.4 T, I_p = 190 kA, n_e = 1.3 x10^{19} m^{-3}) the potential measured at r = 0.21 - 0.27 m was negative. The profiles presented in Fig. 5 were obtained with a single spatial scan of HIBP with beam energy E_b = 240 keV. Corresponding temporal evolution in the deepest point of the scan are also shown. The potential profile presents linear-like function with the lowest absolute value at the deepest point $\varphi(0.21)$ = –600 V. The slope of the potential profile gives the estimation of the mean radial electric field E_r ~ - 6.7 kV/m. In the ECRH phase of the discharge (on-axis heated plasmas with P_{EC} ~0.4 MW) the absolute potential well becomes significantly smaller, $\varphi(0.21)$= –210 V, and the electric field decreases to E_r ~ -2.3 kV/m. A clear link between the core plasma potential and ECRH power was observed: the stronger power leads to the higher (more positive) absolute potential. This tendency found first earlier [7] was also obtained in TJ-II stellarator during experiments with the ECRH power modulation [8].

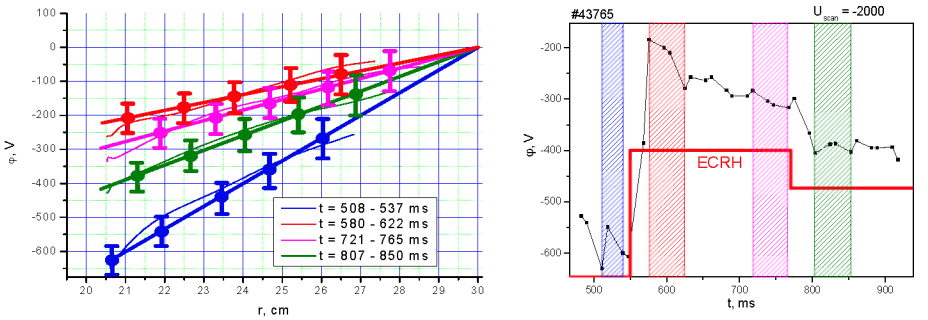

FIGURE 5. Left: single scan profiles during the OH phase (blue) and the ECRH phases with two (red and magenta) and one (green) gyrotron operating. Right: evolution of plasma potential at the deepest measuring location (r_{min}=21 cm).

For the present plasma conditions and radial range of the HIBP measurements, Er ~ const, the plasma column rotates not as a rigid body due to the B(r) dependence. The typical values $\mathbf{V_{E\times B}}$ ~ 3.0 km/s, $\mathbf{\Omega_{E\times B}}$ ~ $1.5*10^4$ radian/s for the Ohmic stage and $\mathbf{V_{E\times B}}$ ~ 2.4 km/s $\mathbf{\Omega_{E\times B}}$ ~ $1.25*10^4$ radian/s for the ECRH stage.The turbulence rotation velocities were measured by correlation reflectometry (CR) during the same discharges. The experimental layout is shown in Fig 6. CR antennae are located 90 degree anticlockwise from HIBP along the torus. E×B drift velocity $\mathbf{V}_{E\times B} = E_r/B_{tor}$ was taken by E_r, obtained by HIBP, and B_{tor} for the x coordinate, corresponding to the CR measurements. The absolute values of the angular rotation velocity $\mathbf{\Omega_{TURB}}$ are close to the plasma drift rotation velocity $\mathbf{\Omega_{E\times B}}$, see Fig 7. $\mathbf{\Omega_{TURB}}$ shows the radial dependence in consistency with $\mathbf{\Omega_{E\times B}}$ rotation. Both velocities decrease accordingly when ECRH applied. Within the achieved experimental accuracy turbulence tends to rotate with plasma ExB rotation velocity. To clarify the link between the plasma drift

rotation and turbulence rotation more work should be done, specifically at the plasma periphery, where CR and HIBP measurements differs to each other.

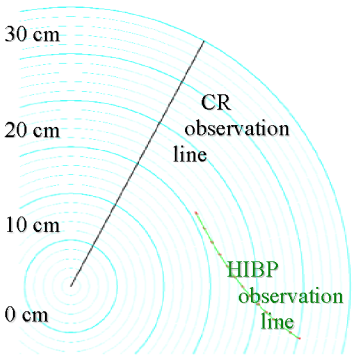

FIGURE 6. Experimental layout for comparative rotation measurements.

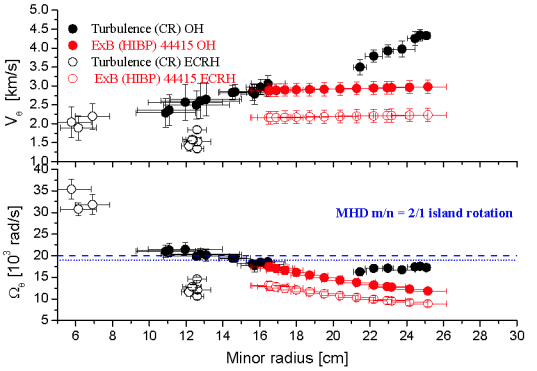

FIGURE 7. Comparison of rotation velocities of density perturbations with core plasma rotation in OH and ECRH plasma

CONCLUSIONS

Using dedicated probe arrays and fast bolometry the structure of electrostatic turbulence in the edge plasma of the CASTOR tokamak , as well as the radial profile of the radial electric field and of the poloidal and toroidal flows have been clearly identified in OH and electrode-biased discharges. Advanced HIBP and reflectometry on the tokamak T-10 allowed to determine radial plasma potential profiles in OH and ECRH discharges as a function of density, and to show that the turbulence rotation velocity is consistent with the ExB velocity.

ACKNOWLEDGMENTS

This research has been partially supported by the Grant Agency of the Academy of Sciences of the Czech Republic (grant KJB100430504). Kurchatov team was supported by Goscontract RF 02.516.11.6068 and Grants RFBR 05-02-17016, 07-02-01001, INTAS 100008-8046, NWO-RFBR 047.016.015. Attendance to the JE's was partially supported through IAEA and ICTP grants.

REFERENCES

1. M. Gryaznevich et al., Nucl. Fusion 45 (2005) 245
2. G.Van Oost et al., Nucl. Fusion 47 (2007) 378
3. P. Peleman et al.,, J. Nucl. Mater. 363-365 (2007) 638
4. E.Dufkova et al., 32nd EPS Conf. on Plasma Phys (Tarragona, 2005) vol.29 (ECA) P-2.074
5. S.V. Perfilov et al., 34th EPS Conf. on Plasma Phys (Warsaw, 2007)
6. Vershkov V A et al. Nucl. Fusion 45 (2005) 203
7. A.V.Melnikov et al., 32nd EPS Conf. on Plasma Phys (Tarragona, 2005) vol.29 (ECA) P-4.089
8. L.I.Krupnik et al., 31st EPS Conf. on Plasma Phys (London, 2005) vol.28 (ECA) P-4.089